Ultrasonics - Sonochemistry 64 (2020) 105042

Contents lists available at ScienceDirect

Ultrasonics - Sonochemistry

journal homepage: www.elsevier.com/locate/ultson

Ultrasound-assisted regeneration of zeolite/water adsorption pair

Hooman Daghooghi-Mobarakeh[a], Nicolas Campbell[b], Weston K. Bertrand[a], Praveen G. Kumar[c], Sumit Tiwari[d], Liping Wang[a], Robert Wang[a], Mark Miner[e], Patrick E. Phelan[a,*]

[a] School for Engineering of Matter, Transport & Energy, Arizona State University, Tempe, AZ 85287-6106, USA
[b] Polytechnic School, Arizona State University, Mesa, AZ 85212-5880, USA
[c] CO_2 Research and Green Technologies Centre, Vellore Institute of Technology, Vellore, Tamil Nadu 632014, India
[d] School of Engineering, Shiv Nadar University, Greater Noida, Uttar Pradesh 201314, India
[e] School of Earth and Space Exploration, Arizona State University, Tempe, AZ 85287-6305, USA

ARTICLE INFO

Keywords:
Ultrasound
Zeolite
Desorption
Regeneration
Thermal storage
Sorption cooling

ABSTRACT

The use of ultrasound to enhance the regeneration of zeolite 13X for efficient utilization of thermal energy was investigated as a substitute to conventional heating methods. The effects of ultrasonic power and frequency on the desorption of water from zeolite 13X were analyzed to optimize the desorption efficiency. To determine and justify the effectiveness of incorporating ultrasound from an energy-savings point of view, an approach of constant overall input power of 20 or 25 W was adopted. To measure the extent of the effectiveness of using ultrasound, the ultrasonic-power-to-total power ratios of 0.2, 0.25, 0.4 and 0.5 were investigated and the results compared with those of no-ultrasound (heat only) at the same total power. To analyze the effect of ultrasonic frequency, identical experiments were performed at three nominal ultrasonic frequencies of ~28, 40 and 80 kHz. The experimental results showed that using ultrasound enhances the regeneration of zeolite 13X at all the aforementioned power ratios and frequencies without increasing the total input power. With regard to energy consumption, the highest energy-savings power ratio (0.25) resulted in a 24% reduction in required input energy and with an increase in ultrasonic power, i.e. an increase in acoustic-to-total power ratio, the effectiveness of applying ultrasound decreased drastically. At a power ratio of 0.2, the time required for regeneration was reduced by 23.8% compared to the heat-only process under the same experimental conditions. In terms of ultrasonic frequency, lower frequencies resulted in higher efficiency and energy savings, and it was concluded that the effect of ultrasonic radiation becomes more significant at lower ultrasonic frequencies. The observed inverse proportionality between the frequency and ultrasound-assisted desorption enhancement suggests that acoustic dissipation is not a significant mechanism to enhance mass transfer, but rather other mechanisms must be considered.

1. Introduction

Desiccants consisting of solid porous materials are increasingly gaining attention for various applications including thermal energy storage, sorption cooling, dehumidification processes, water purification, desalination, and water harvesting [1–6]. One of the significant drawbacks of using desiccant materials is the lengthy and energy-inefficient process of regeneration of the material, which calls for novel and more efficient desorption processes instead of conventional regeneration processes namely direct heating and application of hot air [7]. Zeolite 13X is porous crystalline alumina silicate with maximum water adsorption capacity of 12% – 36% by mass [8,9]. As a desiccant material, zeolite 13X has various applications including sorption cooling [9–13] and thermal storage [14–16]. Wang et al. [11] reported the adsorption enthalpy of the zeolite-water pair to be about 3300–4200 kJ/kg and the regeneration temperature to be about 250–300 °C. The high values of adsorption enthalpy and regeneration temperature of the zeolite/water pair, compared to other adsorption pairs like silica gel/water or activated carbon/ammonia, makes it both a curse and a blessing for sorption cooling and thermal storage applications, respectively. In recent years researchers have attempted to resolve the issue of inefficiencies caused by inadequate heat and mass transfer in desiccant materials by introducing alternative energy sources to assist in the desorption process along with low-grade heating [17,18]. One such energy source is ultrasound [7,19–23]. Ultrasound has been used to not only assist desorption of adsorbates in sorption

* Corresponding author.
E-mail address: phelan@asu.edu (P.E. Phelan).

https://doi.org/10.1016/j.ultsonch.2020.105042
Received 28 November 2019; Received in revised form 12 February 2020; Accepted 21 February 2020
Available online 22 February 2020
1350-4177/

Nomenclature

α_p	acoustic attenuation in porous media (dB cm^{-1})
α_s	acoustic attenuation in solid (dB cm^{-1})
α_v	acoustic attenuation in void (dB cm^{-1})
δ	acoustic diffusivity (m^2 s^{-1})
θ	phase angle (Rad)
$\Delta m_{removed,US}$	mas of adsorbate removed with ultrasound (g)
$\Delta m_{removed,non\ US}$	mas of adsorbate removed without ultrasound (g)
Δt	time period (s)
A	adsorption Potential (J)
A_s	material specific coefficient (m^{-3} s^4)
C_0	Speed of sound (m s^{-1})
D	grain diameter (m)
f_{US}	ultrasonic frequency (Hz)
I_{rms}	root mean square current (A)
MR	moisture ratio (–)
m_{dry}	mass of dry sample (g)
$m_{measured}$	measured mass (g)
P	pressure (kPa)
P_s	saturation pressure (kPa)
P_{TH}	thermal power (W)
P_{US}	ultrasonic power (W)
R	ideal gas constant (J mol^{-1} k^{-1})
T	temperature (°k)
T_{reg}	regeneration temperature (°C)
TH	Thermal (–)
UDE	ultrasonic desorption enhancement (–)
$UDEE$	ultrasonic desorption efficiency enhancement (–)
US	Ultrasound (–)
V_{rms}	root mean square voltage (V)

cooling, but also desorption of many other chemicals as well as the drying of food, clothing and wood [24–35]. The use of ultrasound on adsorbents has been recently studied as a means of overcoming insufficient heat and mass transfer during the regeneration of the adsorbents. Conventional heating of adsorbents is the primary contributor to the long time required for regeneration and the energy-consuming nature of the desorption process. In the relatively sparse amount of research available on ultrasonic regeneration, there have been investigations on the effect of the input power and frequency of the sound waves as well as on how those inputs perform under different thermal power input, e.g., regeneration temperature [7,22,23]. Zhang et al. [23] investigated the effects of different levels of ultrasonic power and regeneration temperature on moisture removal from silica gel and found that higher ultrasonic power and regeneration temperature results in higher desorption. Zhang et al. [22], on the other hand, investigated the effects of ultrasonic frequency on moisture removal from silica gel. They reported that with an increase in ultrasonic frequency desorption decreases. These studies have attributed numerous theories on ultrasonic interaction with silica gel for a fundamental explanation as to why desorption is enhanced. But, as discussed below, the fundamental mechanisms behind why the application of ultrasound improves desorption are still not clear.

In recent years there have been several efforts to conceptualize the principle of ultrasound-enhanced desorption. This improved desorption process can be described using heat and mass transfer governing relations while also incorporating ultrasonication effects to analyze this improvement [36]. In the literature, there are several contributing factors cited proposing why improved desorption occurs due to the introduction of an acoustic field, but the most common factor discussed in previous studies is *surface cavitation* [25,36–41]. The alternating, locally established compressions and rarefactions induced by ultrasound waves at the surface of the adsorbent material subject the solid-gas interface to successive higher and lower pressures. Experimentally, it has been shown that the effect of expansion dominates that of compression at the interface, which results in surface cavitation that breaks the boundary layer and overcomes the adsorption forces (van der Waals forces) [37]. Another important effect of ultrasound that improves desorption that has been discussed is ultrasonic-induced, locally established partial vacuum. When an adsorbent is under ultrasonic radiation, a pulsating partial vacuum is created at the same frequency of the ultrasonic field that in turn reduces the gas pressure at the gas-solid interface and enhances vapor transport by canceling or prevailing over the present adsorption field and thus promoting surface evaporation [25,37,39]. Based on findings from previous studies, another factor shown to play a significant role in ultrasound-assisted desorption is circulating fluid currents. Induced by high-intensity ultrasonic radiation at the adsorbent surface, circulating currents enhance desorption of adsorbate from the surface [42]. The movement of the adsorbate molecules is achieved when acoustic forces dominate the viscous and surface forces allowing molecules to move more freely. This phenomenon is also reported as *microstreaming*, which occurs at the desiccant material surface resulting in a reduction in the diffusion boundary layer hence an increase in diffusion and mass transfer [38]. Another explanation proposed is that the alternating pressure creates local vapor bubbles, which force liquid molecules to move around forming currents [25]. It has also been postulated that the flow of the fluid in porous media is accelerated in an ultrasonic field [25,43]. Turbulence is another factor contributing to ultrasonic-enhanced desorption. Turbulence induced at the gas phase will partially reduce the gas pressure and consequently increase the diffusivity at the gas-solid interface [37]. Viscosity and diffusivity are important factors governing the heat and mass transfer and must be considered in any discussion of enhanced desorption. Ultrasonic radiation reduces the adsorbate viscosity, which will have the effect of increasing its diffusivity [44,45]. The temperature rise due to dissipation of ultrasonic energy is a controversial factor. In some studies, the application of ultrasonic waves has been considered as a contributing factor to enhanced mass transfer, while in others dismissed as a contributing factor compared to others [37,44].

At this point, it seems the precise mechanisms by which ultrasound enhances desorption from porous media are not firmly established. In the previous studies [22,23,46], ultrasound was applied along with thermal power, but the total power (heat + ultrasound) was not kept constant. Although integration of ultrasound appeared to be beneficial, the total efficiency of the process was not clear because the total power added to the adsorbent increased with the addition of ultrasound. The aim of this paper, therefore, is to investigate the extent to which integration of ultrasound is beneficial from an energy-savings point of view. In other words, the novelty of this study is to *address the concern of energy efficiency*: if a portion of the thermal power is replaced with acoustic power while the total input power to the system is constant, is the addition of ultrasound still beneficial? In addition, comparing the simultaneous desorption rate and regeneration temperature of both heat-only and heat + ultrasound desorption processes makes it possible to accredit or discredit some of the proposed mechanisms of ultrasound-enhanced desorption.

2. Material and experimental setup

2.1. Zeolite 13X

The zeolite 13X beads used in this study were procured from SORBENT SYSTEMS IMPAK Inc. The physical properties and specifications provided by the supplier are presented in Table 1.

Table 1
Physical Properties of zeolite 13X.

Bead diameter (mm)	3–5
Pore diameter (nm)	1.3
Specific surface area (m^2/g)	726
Porous volume (ml/g)	0.25
Density (kg/m^3)	689

2.2. Experimental procedure

The main components of the experimental equipment used in this study are the desorption bed, an ultrasonic transducer, a function generator (Siglent Technologies SDG1032X), a high frequency-low slew rate amplifier (AALABSYSTEMS A-303), a cartridge heater, and a power supply (PROTEK P6000). A detailed schematic of the experimental setup is shown in Fig. 1. The bed is of hollow cylindrical shape machined out of aluminum 6061 rod. The ultrasonic transducers used are of low-heat piezoceramic type procured from APC INTERNATIONAL. Incorporating a combination of function generator and amplifier instead of fixed power - frequency ultrasonic generator makes it possible to drive the transducer at any desirable power level and frequency. The desorption bed is attached to the transducer with resin epoxy. A detailed photo of the experimental setup is also provided in Fig. 1. Drying of the zeolite sample was achieved by heating it in an oven at 280 °C and measuring the mass until no change in mass was observed. The drying process of the sample was validated using a vacuum oven. The mass of the dried sample was controlled to be 48.31 ± 0.01 g in all experiments. The dried sample was then saturated to 27% moisture ratio (*MR*) using an ultrasonic humidifier. During the saturation stage, the relative humidity and the temperature of the feed flow were controlled at 95%-100% and 20 °C respectively using a Honeywell HIH-6130 temperature and relative humidity sensor. The moisture ratio, representing the mass of water adsorbed by zeolite 13X, is used to describe the desorption process and is defined as:

$$MR = \frac{M_{measured} - M_{dry}}{M_{dry}} \quad (1)$$

where $M_{measured}$ is the measured mass of the sample and M_{dry} the measured mass of the dry sample. The resonant frequency of the transducers was determined using an oscilloscope (Rigol DS 1054Z) and a shunt resistor.

The ultrasonic transducer and the shunt resistor were connected in series and with the help of four voltage probes, the impedance of the transducer based on the voltages across the transducer and across the shunt resistor was calculated. The resonant frequency corresponds to the lowest impedance (also the phase difference between the voltage and current is zero) [47]. The resonant frequencies of the unloaded transducers provided by the supplier, 28 kHz (APC 90–4040), 40 kHz (APC 90–4050), and 80 kHz (APC 90–4040) kHz were validated and the resonant frequency of the transducer-bed assembly was measured to be 24.3, 31.5, and 75.5 kHz, respectively. Identically, for each frequency, experiments at two levels of total power (P_{Total} = 20 and 25 W) were carried out. The experimental ultrasonic (P_{US}) – thermal power (P_{TH}) combinations are presented in Table 2. Thermal power was regulated through a power supply connected to the cartridge heater. The ultrasonic power was regulated using a shunt resistor, an oscilloscope and voltage probes. The ultrasonic power was determined as:

$$P_{US} = V_{rms} I_{rms} \cos\theta \quad (2)$$

where V_{rms} is the root mean square value of voltage across the transducer, I_{rms} the root mean square value of alternating current passing through the transducer, and θ the phase angle between the voltage and current.

Since zeolite 13X is a poor heat conductor, the regeneration temperature was measured at three different locations using OMEGA T type thermocouples (wire diameter = 0.571 mm), referred to as reference,

Table 2
Experimental ultrasonic-thermal power combinations.

P_{Total} (W)	P_{TH} (W)	P_{US} (W)	P_{US}/P_{Total} (W)
20	20	0	0
20	15	5	0.25
20	10	10	0.50
25	25	0	0
25	20	5	0.20
25	15	10	0.40

Table 3
Accuracy of measured variables.

Measured variable	Accuracy	Unit
Temperature	± 1.0	°C
Mass	± 0.01	g
Voltage	2	%
Phase angle	0.1	minute

Table 4
Maximum values of uncertainty for calculated variables.

Calculated variable	Maximum uncertainty	unit
MR	± 0.21	%
T_{reg}	± 1.7	°C
UDE	± 0.45	%
UDEE	± 1.98	%

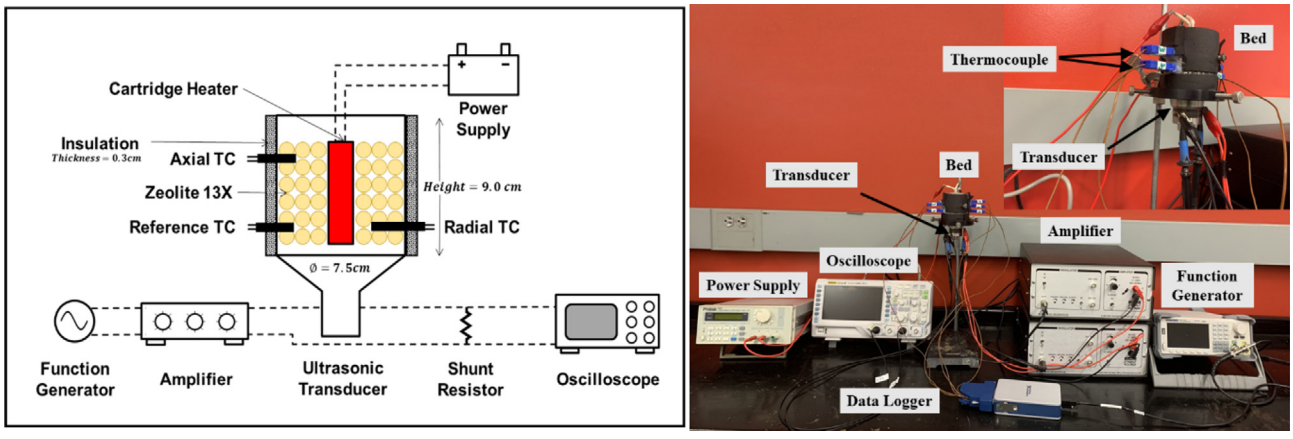

Fig. 1. Schematic diagram (left) and detailed photo (right) of the experimental setup.

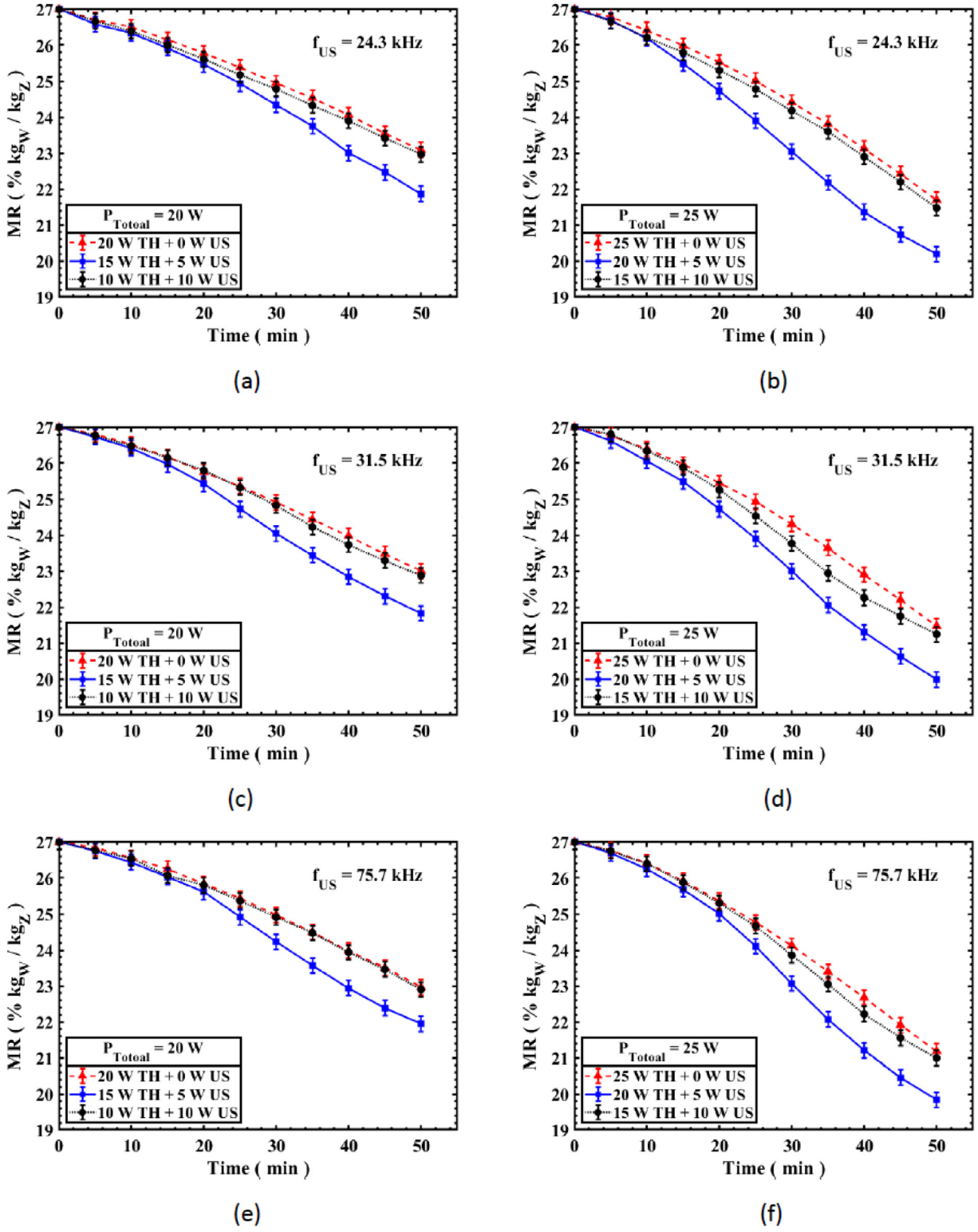

Fig. 2. Desorption curves for zeolite/water. (a) at 24.3 kHz and 20 W; (b) at 24.3 kHz and 25 W; (c) at 31.5 kHz and 20 W;(d) at 31.5 kHz and 25 W; (e) at 75.7 kHz and 20 W; (f) at 75.7 kHz and 25 W.

axial, and radial temperatures, and a NATIONAL INSTRUMENTS data acquisition device NI 9212. The reference and axial thermocouples are positioned at the same radial distance (20 mm) from the center of the bed and at 5 mm and 25 mm axial distance from the inner bottom surface of the bed, respectively. The radial thermocouple is positioned at the same axial height (5 mm) as the reference thermocouple and at a radial distance of 15 mm from the center of the bed. The placement of thermocouples is such that an average adsorption bed temperature can be measured, but the positional accuracy of the thermocouples is not sufficient to determine radial and axial temperature gradients. The experimental period is limited to 50 min and the mass and temperatures are measured at 5-minute intervals. For each measurement, all wires are disconnected from the bed and the mass of the bed is measured using an electronic scale (My Weigh SCMIM01) with a capacity of

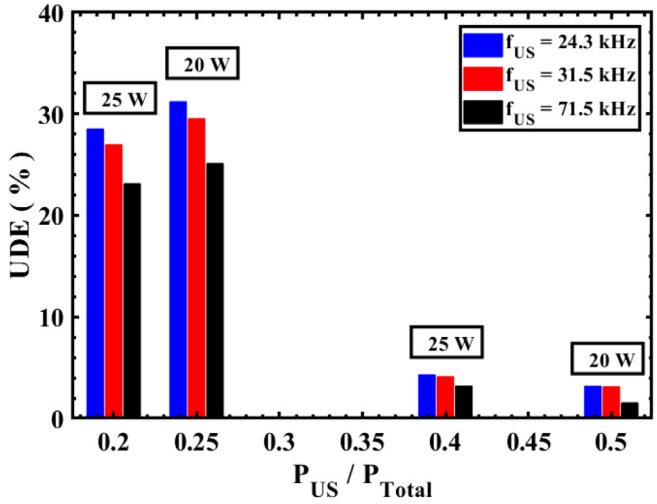

Fig. 3. Ultrasonic desorption enhancement for zeolite / water at different frequencies and total power levels. The uncertainty of the UDE is provided in Table 4.

1000 ± 0.01 g.

2.3. Ultrasonic desorption enhancement

The ultrasonic desorption enhancement *UDE* indicates the percent improvement in removing the adsorbate (here, water) using ultrasound compared to a heat-only desorption process and is defined as:

$$UDE = \frac{\Delta m_{removed,US} - \Delta m_{removed,nonUS}}{\Delta m_{removed,nonUS}} \quad (3)$$

where $\Delta m_{removed,US}$ is the mass of adsorbate (water) removed in a desorption process involving ultrasound and $\Delta m_{removed,non\ US}$ is the mass of adsorbate (water) removed in a heat-only desorption process.

2.4. Ultrasonic desorption efficiency enhancement

The ultrasonic desorption efficiency enhancement *UDEE* is an indicator of the amount of energy saved in desorbing adsorbate (water) from the adsorbent (zeolite 13X) by using ultrasound compared to a heat-only desorption process and is defined as:

$$UDEE = \frac{\frac{P_{Total}\Delta t}{\Delta m_{removed,nonUS}} - \frac{P_{Total}\Delta t}{\Delta m_{removed,US}}}{\frac{P_{Total}\Delta t}{\Delta m_{removed,nonUS}}} \quad (4)$$

where Δt is the total time of the experiment (50 min). The common numerator $P_{Total}\Delta t$ was not cancelled to keep the universality and a sense of specific energy in the equation.

2.5. Uncertainty analysis

2.5.1. Measured and explanatory variables

The thermocouple-data acquisition device was calibrated using a HONEYWELL HIH 6130 Silicon bandgap temperature sensor with an accuracy of ± 1.0 °C. The accuracies of the mass and temperature measurements are provided in Table 3.

The uncertainties of the calculated variables were determined using [48]

$$w_f = \left(w_1^2 \left(\frac{\partial f}{\partial x_1}\right)^2 + w_2^2 \left(\frac{\partial f}{\partial x_2}\right)^2 + w_3^2 \left(\frac{\partial f}{\partial x_3}\right)^2 + \cdots \right)^{0.5} \quad (5)$$

where w_f is the uncertainty of the calculated variable $f(x_1, x_2, x_3,\ldots)$ and $w_1, w_2, w_3, \ldots$ the uncertainties involved in the measured variables $x_1, x_2, x_3,\ldots$ respectively.

For instance, the uncertainty associated with the calculated variable *MR* is obtained using

$$w_{MR} = \sqrt{w_{m_{measured}}^2 \left(\frac{1}{m_{dry}}\right)^2 + w_{m_{dry}}^2 \left(\frac{m_{measured}}{m_{dry}^2}\right)^2} \quad (6)$$

The maximum values of uncertainty of the calculated variables are provided in Table 4.

2.5.2. Sensible heat losses

To minimize the effects of sensible heat losses, the desorption bed was fully insulated. However, some amount of heat loss is unavoidable and should be taken into consideration in interpreting the experimental results. To investigate the amount of heat losses and for the purpose of comparing the sensible heat loss to the heat gained by the zeolite, the worst case heat loss, i.e., the maximum temperature rise (15 W thermal power and 10 W of ultrasound at nominal frequency of 80 kHz) is considered. Since the bed is a short, thick cylinder, the effect of curvature can be neglected and the periphery is regarded as a vertical surface [49]. The top surface of the bed is treated as a horizontal surface. Assuming natural convection from the horizontal and vertical surfaces and using the known temperatures of the insulation surface and the ambient, the heat transfer coefficients for vertical and horizontal surfaces are evaluated to vary between 0.24 and 5.72 W m^{-2} K^{-1} and 6.51–11.3 W m^{-2} K^{-1} throughout the experiment, respectively. The total average heat loss for the entire period of the experiment is ~1.8 W corresponding to 7.2% of the total input power.

2.5.3. Bed size and input power proportionality

Since this work is a comparative study that evaluates and justifies the energy-saving characteristic of ultrasound–assisted versus heat-only desorption, and considering that the sensible heat losses are taken into account, the size of the desorption bed is not of importance. However, to realize the real–time applicability of the study, the amounts of input power are proportional to the bed size. The specific cooling power of the zeolite-water pair is reported to be about 200–600 W kg^{-1} [9,13], so the 20 and 25 W of total input power corresponding to specific desorbing input powers of 327 and 410 W kg^{-1} respectively, are comparable.

3. Results and discussion

3.1. Moisture ratio

Fig. 2 shows the reduction in moisture ratio (i.e. desorption) of zeolite 13X for all six power combinations and at all three ultrasonic frequencies, including no applied ultrasound (heat-only). It can be observed from the figure that with constant power level, replacing some portion of thermal power with ultrasound enhances moisture removal from the adsorbent. In previous studies [7,22,23], the ultrasound was added to the thermal power such that the total power increased from the heat-only experiments to the ones with ultrasound. Although this approach confirms that applying ultrasound enhances desorption, the fact that heat-only and ultrasound-assisted experiments were not performed with the same level of total power makes it impossible to justify the use of ultrasound in terms of energy savings. The novelty of the present study is the *constancy of total power in both heat-only and ultrasound-integrated experiments* that justifies the use of ultrasound to enhance the desorption process.

Since the total input power is constant, the enhancement in desorption must be ultrasound related. The highest moisture ratio in this study is 27% meaning that the total mass of adsorbed water is 13.04 g. Using water molar mass and Avogadro's number, there are a total of 4.36×10^{23} water molecules present. Assuming a uniform adsorptive distribution (water molecules tend to adhere to the zeolite surfaces rather than to other water molecules), and considering a water

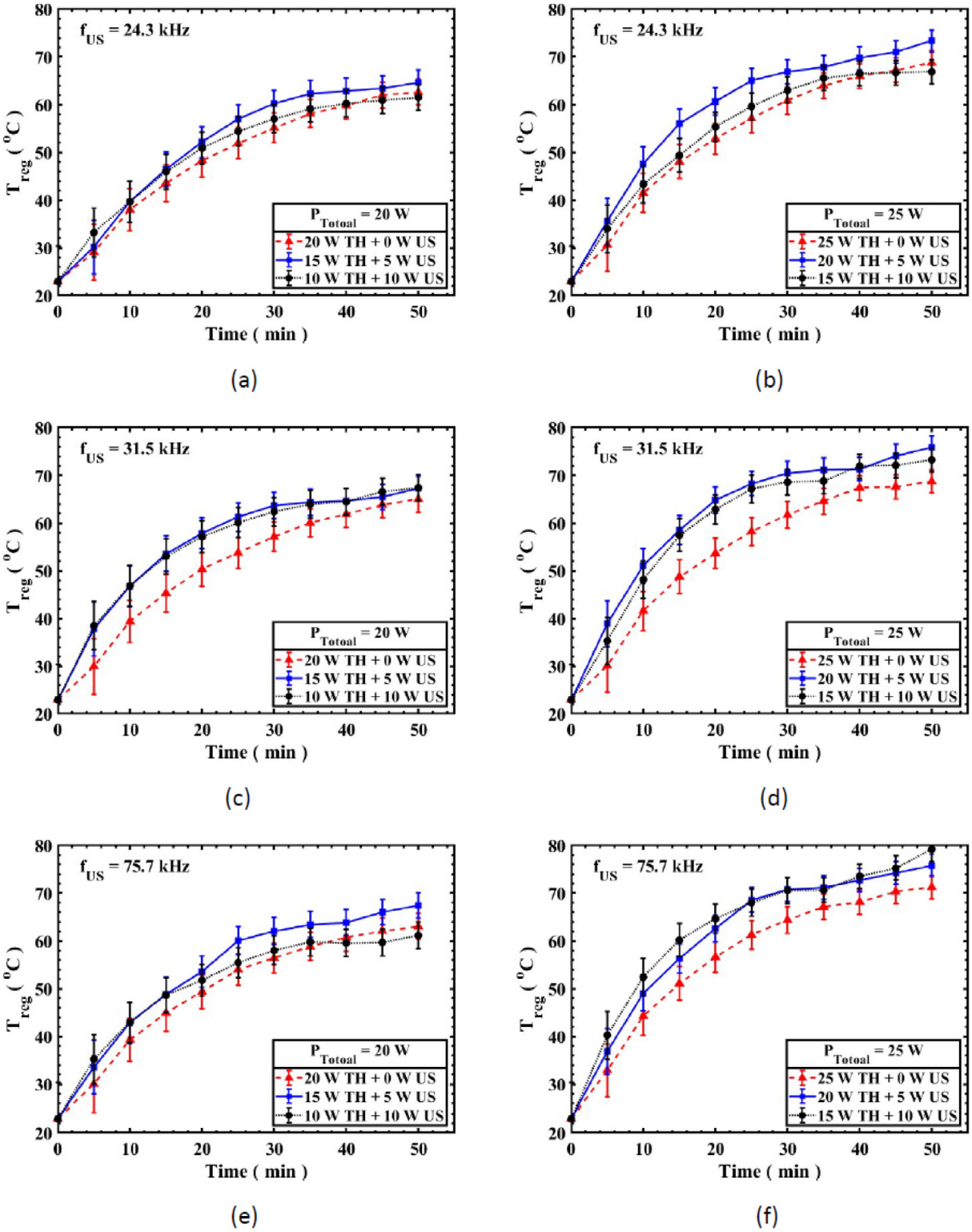

Fig. 4. Desorption curves for zeolite/water. (a) at 24.3 kHz and 20 W; (b) at 24.3 kHz and 25 W; (c) at 31.5 kHz and 20 W;(d) at 31.5 kHz and 25 W; (e) at 75.7 kHz and 20 W; (f) at 75.7 kHz and 25 W.

molecule effective radius of 0.097 nm, the total surface occupied by water molecules is 12.64×10^3 m^2. The mass of dry zeolite sample is 48.31 g, and using the sample's specific area of 726 m^2/g, the total surface of the zeolite sample is 35.07×10^3 m^2. The average *surface coverage* is therefore obtained as

$$Surface\ coverage = \frac{A_{water,Total}}{A_{zeolite,Total}} = \frac{12.64 \times 10^3}{35.07 \times 10^3} = 0.36 = 36\% \quad (7)$$

In case of non-uniform adsorption of water molecules resulting in water cluster formation (which usually occurs in hydrophobic adsorbents), the size of the water molecule accumulation is reported not to exceed a pentamer [50–52]. Considering both uniform and non-

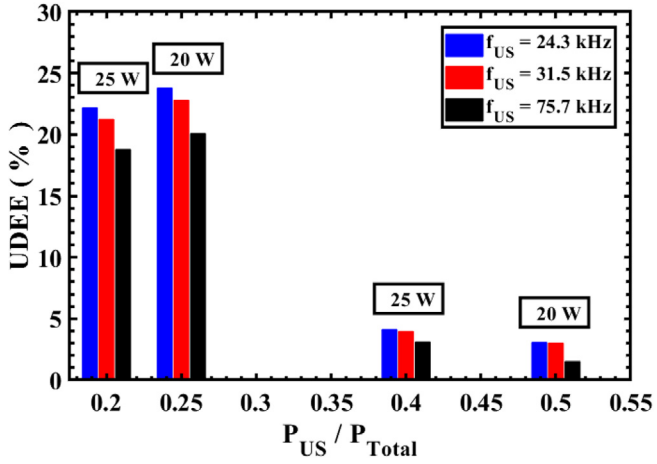

Fig. 5. Ultrasonic desorption efficiency enhancement for zeolite/water at different frequencies and total power levels. The uncertainty of the UDEE is provided in Table 4.

Table 5
Elapsed regeneration time at 24.3 kHz ultrasonic frequency.

Total power (W)	Power ratio	Final moisture ratio (%)	Time (min)
20	0.00	23.09	50.0
	0.25		40.8
	0.50		48.4
25	0.00	21.70	50.0
	0.20		38.1
	0.40		48.3

Table 6
BET analysis of the zeolite sample before and after ultrasonication.

Characteristic	Before	After
Specific surface area (m^2/g)	480.4843	463.4843
Porous volume (ml/g)	0.2223	0.2136
BJH Desorption average pore width (nm)	8.4955	8.4623

uniform adsorptive distribution scenarios, we can confidently conclude that neither bulk liquid nor bulk-imitating liquid clusters exist in our sample. In the absence of bulk liquid or liquid film, the effects of ultrasonication involving liquid including the viscosity effect, capillary effect, sonic currents, microstreaming, circulating flow and surface cavitation can be disregarded. The observed ultrasound-assisted enhancement in desorption is therefore perhaps due to ultrasound-induced establishment of local partial vacuum and alternating zones of compression and rarefaction resulting in enhanced mass diffusivity. Another potential mechanism worth mentioning is the effect of turbulence. The ultrasound-triggered pressure alteration causes turbulence resulting in an increase in mass diffusivity. The same effect is observed in Henry's constant in acoustic fields [44].

3.1.1. Effect of ultrasonic power

Although ultrasonic radiation apparently improves the desorption process, the amount of ultrasonic power to be used in order to achieve the highest desorption at the lowest total power input is of major concern. A closer look at Fig. 2 reveals that at any frequency, for the 20-W total power experiments, the highest desorption was achieved with a power combination of 15 W thermal power and 5 W of ultrasonic power, i.e., a ratio of ultrasonic-to-total power of $P_{US}/P_{Total} = 0.25$. In addition, with an increase in this power ratio to 0.50, there is still a slight enhancement in desorption compared to the heat-only experiment but it is relatively insignificant. The same trend, regardless of variation in frequency, can be observed for the 25-W total power experiments. The greatest enhancement in desorption occurred at a power combination of 20 W thermal and 5 W of ultrasonic power ($P_{US}/P_{Total} = 0.20$). Again, at a higher $P_{US}/P_{Total} = 0.40$, there is a modest improvement in desorption over the heat-only experiment. This suggests that there is an optimal value for P_{US}/P_{Total} resulting in maximal adsorbate removal per constant total power.

3.1.2. Effect of ultrasonic frequency

The values of ultrasonic desorption enhancement *UDE* relative to heat-only desorption are plotted in Fig. 3. It can be concluded from the figure that for any total power level and with any ultrasonic – thermal power combination, with an increase in ultrasonic frequency f_{US}, the ultrasonic desorption enhancement decreases. The same trend of deterioration in desorption enhancement with an increase in f_{US} has been observed in some previous studies [22]. The reduction is somehow proportional to the increase in f_{US}. With a slight shift from 24.3 kHz to 31.5 kHz, there is a slight drop in *UDE*. However, with an increase from 24.3 kHz to 75.7 kHz, there is a significant reduction in *UDE*. The inverse proportionality between f_{US} and *UDE* in some ways appears to confirm the ultrasound-induced desorption improvement through partial vacuum and zones of alternating pressure. At higher frequencies, the rarefication, compression, and partial vacuum are established and demolished so fast that there may not be enough time for the mass-transfer-enhancing effects to be fully developed. The same phenomena can be observed in ultrasonic-induced cavitation when acoustic-induced cavitation bubbles explode prematurely at higher frequencies [53,54].

Additionally, this inverse proportionality between desorption and ultrasonic frequency which has also been reported in the literature [22], contradicts the proposed theory of ultrasound-enhanced desorption through acoustic dissipation [36] to some degree since the acoustic attenuation coefficient is proportional to frequency. An increase in frequency should therefore lead to an increase in desorption [55–57], but that is contradicted by the current results. The attenuation in porous media can be thought of as an amalgamation of attenuation in the solid and void parts. The attenuation in the granular solid part α_s is defined as [58]:

$$\alpha_s = A_s D^3 f_{US}^4 \tag{8}$$

where A_s is a material-specific coefficient that depends on the elastic moduli, D the grain diameter and f the frequency of the acoustic wave. The attenuation in the void part regardless of the presence of adsorbate molecules is thermoviscous absorption and is formulated as [59]:

$$\alpha_v = \frac{2\pi^2 \delta f_{US}^2}{C_0^3} \tag{9}$$

where δ is the fluid-specific acoustic diffusivity and c_0 the speed of sound in the fluid media. Thus the acoustic attenuation in porous media, regardless of the order of predominance, depends on f_{US} to either the 2nd or 4th power:

$$\alpha_p \propto F(f_{US}^4, f_{US}^2) \tag{10}$$

Therefore, it appears unlikely that increased acoustic dissipation is responsible for the observed enhancements in desorption.

3.2. Regeneration temperature

Fig. 4 shows the average regeneration temperature, taken as the average of the three thermocouples shown in Fig. 1, for all experiments.

For all three frequencies and both total power levels, ultrasound-enhanced experiments showed higher temperatures than the non-ultrasonic ones. Specifically, at almost any frequency, the highest temperature was observed at the lower value of P_{US}/P_{Total} meaning that the temperature is not solely dictated by the thermal power and there are

other factors contributing to the temperature rise. One such factor could be the fact that zeolite 13X, being a porous medium with low thermal conductivity (about 0.1–0.6 W m^{-1} $°C^{-1}$) [14], has poor heat transfer capability so using ultrasound enhances the heat transfer in the medium [60–63]. Another reason could be the radially uniform dissipation of ultrasonic waves increasing the temperature rather than relying solely on radial heat conduction from the cartridge heater. The latter cannot be the sole contributor to the temperature rise, as the highest temperature was not observed at higher P_{US}/P_{Total}.

3.3. Ultrasonic desorption efficiency enhancement

The ultrasonic desorption efficiency enhancement *UDEE* indicates the amount of energy saved when a portion of thermal power is replaced with ultrasonic power while the total power remains constant. Fig. 5 shows the percent energy saved for both power levels (20 and 25 W) and at all three levels of frequency. Regarding the ultrasonic frequency f_{US}, there is a general downward trend in *UDEE* with an increase in f_{US}. As can be seen from the figure, there is no distinguishable trend in *UDEE* with regard to P_{US}/P_{Total}. The most efficient desorption process was achieved at $P_{US}/P_{Total} = 0.25$. In addition, with an increase in this ratio, the efficiency drops drastically meaning that there is an optimal ratio of P_{US}/P_{Total} resulting in the highest desorption efficiency enhancement. Considering that desorption is the reverse of the adsorption process, it can be interpreted as overcoming the adsorption potential. Following Polanyi potential theory, the adsorption potential A is defined as [64]:

$$A = RTln\left(\frac{P}{P_s}\right)$$

where R is the ideal gas constant, T the temperature in Kelvin, P the pressure and P_s the adsorbate saturation pressure at T. Keeping in mind that saturation pressure is a function of temperature $f(T)$, the adsorption potential can be rearranged as an implicit function of pressure and temperature H:

$$A = H(T, P)$$

The variation in the pressure is dictated by the ultrasound–induced alternating zones of compression and rarefaction (P_{US}) and the variation in the temperature is imposed by the thermal input (P_{TH}). Therefore, the adsorption potential can be considered as an implicit function of both ultrasonic and thermal inputs H^*:

$$A = H^*(P_{TH}, P_{US})$$

The implicit dependency of adsorption potential on both ultrasonic and thermal input suggests that to achieve the most efficient desorption, the ratio of ultrasonic-to-total power needs to be optimized.

3.4. Desorption speed

In general it is beneficial to reduce the time required for desorption. To investigate the effect of incorporating ultrasound on the desorption speed (i.e., on the time required for desorption), the elapsed times needed for ultrasound-assisted and heat-only regeneration processes to reach the same amount of remaining adsorbed moisture are compared. To do so, for each power level, the water content of the adsorbent at the end of the heat-only experiment (50 min) is considered as the reference value. Then the time needed to reach the same water content in ultrasound-assisted regeneration with the same total power input, is determined. The elapsed times for the most effective frequency (24.3 kHz) are presented in Table 5. The shortest desorption times are observed at $P_{US}/P_{Total} = 0.2$ and 0.25 with 23.8% and 18.4% shorter regeneration processes, respectively. Shifting toward higher P_{US}/P_{Total}, the improvements in desorption time decreases drastically as expected.

3.5. Ultrasonication-induced deterioration

To propose ultrasound as an alternative energy source for regeneration, it is essential to investigate its potential deteriorating and eroding effects.

Although the previous investigations on the subject apparently contradict each other, they suggest that the eroding effects of ultrasonication are associated with its cavitation-inducing nature [65–68]. However, the deteriorating effects of ultrasound on a number of porous materials have been investigated and no significant changes in their sorption capabilities were reported [4,24,69]. In this study, in the absence of bulk liquid, there was no worrisome ultrasound-induced cavitation to be accounted for; however, a BET analysis on a sample after 12 cycles of ultrasonication was carried out to verify the stability of the sample under sonication. The results of the BET analysis for the sample before and after sonication are presented in Table 6. There is a negligible decrease in BET specific surface area, porous volume and pore width that should not affect the adsorption capacity of the sample.

4. Conclusion

In this study, ultrasonic-assisted desorption of water from zeolite 13X was investigated. The extent to which application of ultrasound is effective was analyzed. To do so, the effects of ultrasonic power and ultrasonic frequency on moisture removal and regeneration temperature were investigated. Comparing the moisture ratio at different ultrasonic-to-total power ratios shows that using ultrasound at lower power ratios, i.e. 0.20 and 0.25, significantly improves desorption relative to using only heat for regeneration. Using the newly defined metric *ultrasonic desorption enhancement UDE*, the effects of ultrasonic frequency on moisture removal were analyzed and it was concluded that the effect of ultrasound on desorption is more significant at lower frequencies. Comparing the regeneration temperature of all experiments shows that ultrasonication increases the adsorbent temperature regardless of frequency, presumably due to the heat-transfer-enhancing nature of ultrasound. Not surprisingly, at all three frequencies the highest desorption was achieved at the highest regeneration temperature. Another defined indicator, the *ultrasonic desorption efficiency enhancement UDEE*, was used to justify the use of ultrasound in moisture removal from zeolite 13X. Comparing the values of *UDEE* indicates that with an optimized ratio of ultrasonic-to-total power a ~ 24% reduction in energy and time required for desorption of water from zeolite 13X can be achieved, relative to using only heat.

CRediT authorship contribution statement

Hooman Daghooghi Mobarakeh: Methodology, Investigation, Writing - original draft. **Nicolas Campbell:** Investigation. **Weston K. Bertrand:** Investigation. **Praveen G. Kumar:** Investigation. **Sumit Tiwari:** Investigation. **Liping Wang:** Conceptualization, Funding acquisition, Writing - review & editing. **Robert Wang:** Conceptualization, Funding acquisition, Writing - review & editing. **Mark Miner:** Conceptualization, Funding acquisition, Writing - review & editing. **Patrick E. Phelan:** Conceptualization, Funding acquisition, Writing - review & editing, Supervision.

Declaration of Competing Interest

The authors declare that they have no known competing financial interests or personal relationships that could have appeared to influence the work reported in this paper.

Acknowledgment

This material is based upon work supported by the National Science Foundation under Grant Number CBET – 1703670. Any opinions,

findings, and conclusions or recommendations expressed in this material are those of the authors and do not necessarily reflect the views of the National Science Foundation. The authors would like to thank Ahmad Bamasag from ASU and Alexandre Martin from INSA Rouen who helped in the initial stage of this work.

Appendix A. Supplementary data

Supplementary data to this article can be found online at https://doi.org/10.1016/j.ultsonch.2020.105042.

References

[1] D. Lefebvre, F.H. Tezel, A review of energy storage technologies with a focus on adsorption thermal energy storage processes for heating applications, Renew. Sustain. Energy Rev. 67 (Jan. 2017) 116–125, https://doi.org/10.1016/j.rser.2016.08.019.
[2] A. LaPotin, H. Kim, S.R. Rao, E.N. Wang, Adsorption-based atmospheric water harvesting: impact of material and component properties on system-level performance, Acc. Chem. Res. 52 (6) (Jun. 2019) 1588–1597, https://doi.org/10.1021/acs.accounts.9b00062.
[3] B.N. Bhadra, I. Ahmed, S. Kim, S.H. Jhung, Adsorptive removal of ibuprofen and diclofenac from water using metal-organic framework-derived porous carbon, Chem. Eng. J. 314 (Apr. 2017) 50–58, https://doi.org/10.1016/j.cej.2016.12.127.
[4] S.U. Rege, R.T. Yang, C.A. Cain, Desorption by ultrasound: Phenol on activated carbon and polymeric resin, AIChE J. 44 (7) (Jul. 1998) 1519–1528, https://doi.org/10.1002/aic.690440706.
[5] H. Chen, et al., Toward design rules of metal-organic frameworks for adsorption cooling: effect of topology on the ethanol working capacity, Chem. Mater. 31 (8) (2019) 2702–2706, https://doi.org/10.1021/acs.chemmater.9b00062.
[6] A. Pal, K. Uddin, K. Thu, B.B. Saha, Activated carbon and graphene nanoplatelets based novel composite for performance enhancement of adsorption cooling cycle, Energy Convers. Manage. 180 (2019) 134–148, https://doi.org/10.1016/j.enconman.2018.10.092.
[7] Y. Yao, S. Liu, W. Zhang, Regeneration of silica gel using high-intensity ultrasonic under low temperatures, Energy Fuels 23 (1) (2009) 457–463, https://doi.org/10.1021/ef8000554.
[8] Y. Hirasawa, W. Urakami, Study on specific heat of water adsorbed in zeolite using DSC, Int. J. Thermophys. 31 (10) (2010) 2004–2009, https://doi.org/10.1007/s10765-010-0841-6.
[9] Y.Z. Lu, R.Z. Wang, M. Zhang, S. Jiangzhou, Adsorption cold storage system with zeolite-water working pair used for locomotive air conditioning, Energy Convers. Manage. (2003) 11.
[10] N.C. Srivastava, I.W. Eames, A review of adsorbents and adsorbates in solid–vapour adsorption heat pump systems, Appl. Therm. Eng. 18 (9–10) (1998) 707–714, https://doi.org/10.1016/S1359-4311(97)00106-3.
[11] L.W. Wang, R.Z. Wang, R.G. Oliveira, A review on adsorption working pairs for refrigeration, Renew. Sustain. Energy Rev. 13 (3) (2009) 518–534, https://doi.org/10.1016/j.rser.2007.12.002.
[12] D.C. Wang, Z.Z. Xia, J.Y. Wu, Design and performance prediction of a novel zeolite–water adsorption air conditioner, Energy Convers. Manage. 47 (5) (2006) 590–610, https://doi.org/10.1016/j.enconman.2005.05.011.
[13] S. Vasta, A. Freni, A. Sapienza, F. Costa, G. Restuccia, Development and lab-test of a mobile adsorption air-conditioner, Int. J. Refrig. 35 (3) (2012) 701–708, https://doi.org/10.1016/j.ijrefrig.2011.03.013.
[14] B. Mette, H. Kerskes, H. Drück, H. Müller-Steinhagen, Experimental and numerical investigations on the water vapor adsorption isotherms and kinetics of binderless zeolite 13X, Int. J. Heat Mass Transf. 71 (2014) 555–561, https://doi.org/10.1016/j.ijheatmasstransfer.2013.12.061.
[15] P. Tatsidjodoung, N. Le Pierrès, J. Heintz, D. Lagre, L. Luo, F. Durier, Experimental and numerical investigations of a zeolite 13X/water reactor for solar heat storage in buildings, Energy Convers. Manage. 108 (2016) 488–500, https://doi.org/10.1016/j.enconman.2015.11.011.
[16] S. Semprini, et al., Numerical modelling of water sorption isotherms of zeolite 13XBF based on sparse experimental data sets for heat storage applications, Energy Convers. Manage. 150 (2017) 392–402, https://doi.org/10.1016/j.enconman.2017.08.033.
[17] T. Yamamoto, G. Tanioka, M. Okubo, T. Kuroki, Water vapor desorption and adsorbent regeneration for air conditioning unit using pulsed corona plasma, J. Electrostat. 65 (4) (2007) 221–227, https://doi.org/10.1016/j.elstat.2006.08.002.
[18] T. Chronopoulos, Y. Fernandez-Diez, M.M. Maroto-Valer, R. Ocone, D.A. Reay, Utilisation of microwave energy for CO2 desorption in post-combustion carbon capture using solid sorbents, Energy Proc. 63 (2014) 2109–2115, https://doi.org/10.1016/j.egypro.2014.11.227.
[19] Y. Yao, Enhancement of mass transfer by ultrasound: Application to adsorbent regeneration and food drying/dehydration, Ultrason. Sonochem. 31 (2016) 512–531, https://doi.org/10.1016/j.ultsonch.2016.01.039.
[20] Y. Yao, Research and applications of ultrasound in HVAC field: a review, Renew. Sustain. Energy Rev. 58 (2016) 52–68, https://doi.org/10.1016/j.rser.2015.12.222.
[21] M. Breitbach, D. Bathen, Influence of ultrasound on adsorption processes, Ultrason. Sonochem. (2001) 7.
[22] W. Zhang, Y. Yao, R. Wang, Influence of ultrasonic frequency on the regeneration of silica gel by applying high-intensity ultrasound, Appl. Therm. Eng. 30 (14–15) (Oct. 2010) 2080–2087, https://doi.org/10.1016/j.applthermaleng.2010.05.016.
[23] W. Zhang, Y. Yao, B. He, R. Wang, The energy-saving characteristic of silica gel regeneration with high-intensity ultrasound, Appl. Energy 88 (6) (2011) 2146–2156, https://doi.org/10.1016/j.apenergy.2010.12.023.
[24] O. Hamdaoui, E. Naffrechoux, L. Tifouti, C. Pétrier, Effects of ultrasound on adsorption–desorption of p-chlorophenol on granular activated carbon, Ultrason. Sonochem. 10 (2) (Mar. 2003) 109–114, https://doi.org/10.1016/S1350-4177(02)00137-2.
[25] J.A. Gallego-Juarez, G. Rodriguez-Corral, J.C. Gálvez Moraleda, T.S. Yang, A new high-intensity ultrasonic technology for food dehydration, Drying Technol. 17 (3) (1999) 597–608, https://doi.org/10.1080/07373939908917555.
[26] C. Peng, A.M. Momen, S. Moghaddam, An energy-efficient method for direct-contact ultrasonic cloth drying, Energy 138 (Nov. 2017) 133–138, https://doi.org/10.1016/j.energy.2017.07.025.
[27] J. Kroehnke, G. Musielak, and A. Boratynska, Convective drying of potato assisted by ultrasound, p. 9.
[28] M. Torki-Harchegani, D. Ghanbarian, A. Ghasemi Pirbalouti, M. Sadeghi, Dehydration behaviour, mathematical modelling, energy efficiency and essential oil yield of peppermint leaves undergoing microwave and hot air treatments, Renew. Sustain. Energy Rev. 58 (2016) 407–418, https://doi.org/10.1016/j.rser.2015.12.078.
[29] P. Comandini, et al., Effects of power ultrasound on immersion freezing parameters of potatoes, Innovative Food Sci. Emerg. Technol. 18 (2013) 120–125, https://doi.org/10.1016/j.ifset.2013.01.009.
[30] J.A. Cárcel, J.V. García-Pérez, E. Riera, A. Mulet, Influence of high-intensity ultrasound on drying kinetics of persimmon, Drying Technol. 25 (1) (2007) 185–193, https://doi.org/10.1080/07373930601161070.
[31] S.J. Kowalski, A. Pawłowski, Intensification of apple drying due to ultrasound enhancement, J. Food Eng. 156 (2015) 1–9, https://doi.org/10.1016/j.jfoodeng.2015.01.023.
[32] J. Szadzińska, S.J. Kowalski, M. Stasiak, Microwave and ultrasound enhancement of convective drying of strawberries: Experimental and modeling efficiency, Int. J. Heat Mass Transf. 103 (2016) 1065–1074, https://doi.org/10.1016/j.ijheatmasstransfer.2016.08.001.
[33] K. Schössler, H. Jäger, D. Knorr, Novel contact ultrasound system for the accelerated freeze-drying of vegetables, Innovative Food Sci. Emerg. Technol. 16 (Oct. 2012) 113–120, https://doi.org/10.1016/j.ifset.2012.05.010.
[34] E. Souza da Silva, S.C. Rupert Brandão, A. Lopes da Silva, J.H. Fernandes da Silva, A.C. Duarte Coêlho, P.M. Azoubel, Ultrasound-assisted vacuum drying of nectarine, J. Food Eng. 246 (2019) 119–124, https://doi.org/10.1016/j.jfoodeng.2018.11.013.
[35] Z. He, Y. Fei, Y. Peng, S. Yi, Ultrasound-assisted vacuum drying of wood: effects on drying time and product quality, BioResources 8 (1) (2013) 855–863, https://doi.org/10.15376/biores.8.1.855-863.
[36] Y. Yao, S. Liu, Ultrasonic Technology for Desiccant Regeneration, John Wiley & Sons, Singapore, Singapore, 2014 Incorporated.
[37] R. Penn, E. Yeager, F. Hovorka, Effect of ultrasonic waves on concentration gradients, J. Acoust. Soc. Am. 31 (10) (1959) 1372–1376, https://doi.org/10.1121/1.1907637.
[38] R.S. Soloff, Sonic drying, J. Acoust. Soc. Am. 36 (5) (1964) 961–965, https://doi.org/10.1121/1.1919133.
[39] H.S. Muralidhara, D. Ensminger, Acoustic drying of green rice, Drying Technol. 4 (1) (1986) 137–143, https://doi.org/10.1080/07373938608916315.
[40] P. Greguss, The mechanism and possible applications of drying by ultrasonic irradiation, Ultrasonics 1 (2) (1963) 83–86, https://doi.org/10.1016/0041-624X(63)90059-3.
[41] R.M.G. Boucher, Drying by airborne ultrasonics, Ultrasonic News 3 (2) (1959) 8–16.
[42] H.S. Muralidhara, S.P. Chauhan, N. Senapati, R. Beard, B. Jirjis, B.C. Kim, Electro-acoustic dewatering (EAD) a novel approach for food processing, and recovery, Sep. Sci. Technol. 23 (12–13) (1988) 2143–2158.
[43] J.H. Moy, G.R. Dimarco, Exploring airborne sound in a nonvacuum freeze-drying process, J Food Science 35 (6) (1970) 811–817, https://doi.org/10.1111/j.1365-2621.1970.tb02001.x.
[44] Kiran A. Ramisetty, Aniruddha B. Pandit, Parag R. Gogate, Investigations into ultrasound induced atomization, Ultrason. Sonochem. 20 (1) (2013) 254–264, https://doi.org/10.1016/j.ultsonch.2012.05.001.
[45] V. Fairbanks, W.I. Chen, "Influence of ultrasonics porous media, p. 2.
[46] Y. Yao, W. Zhang, S. Liu, Feasibility study on power ultrasound for regeneration of silica gel—A potential desiccant used in air-conditioning system, Appl. Energy 86 (11) (2009) 2394–2400, https://doi.org/10.1016/j.apenergy.2009.04.001.
[47] A. Arnau (Ed.), Piezoelectric Transducers and Applications, second ed., Springer, New York, 2008.
[48] J.P. Holman, Experimental Methods for Engineers, seveth ed., McGraw-Hill, Boston, 2001.
[49] Y.A. Çengel, A.J. Ghajar, Heat and Mass Transfer: Fundamentals & Applications, fifth ed., McGraw Hill Education, New York, NY, 2015.
[50] D.D. Do, H.D. Do, A model for water adsorption in activated carbon, p. 7, 2000.
[51] T. Iiyama, K. Nishikawa, T. Otowa, K. Kaneko, An ordered water molecular assembly structure in a slit-shaped carbon nanospace, J. Phys. Chem. 99 (25) (1995) 10075–10076, https://doi.org/10.1021/j100025a004.
[52] K. Kaneko, Y. Hanzawa, T. Iiyama, T. Kanda, T. Suzuki, Cluster-Mediated Water Adsorption on Carbon Nanopores, p. 7.
[53] S. Labouret, J. Frohly, Determination of bubble size distributions in an ultrasonic cavitation field, J. Acoust. Soc. Am. 127 (3) (2010) 1984, https://doi.org/10.1121/1.3385105.

[54] S. Merouani, O. Hamdaoui, Y. Rezgui, M. Guemini, Energy analysis during acoustic bubble oscillations: relationship between bubble energy and sonochemical parameters, Ultrasonics 54 (1) (Jan. 2014) 227–232, https://doi.org/10.1016/j.ultras.2013.04.014.
[55] T.L. Szabo, Attenuation, Diagnostic Ultrasound Imaging: Inside Out, Elsevier, 2014, pp. 81–119.
[56] J. Lee, et al., Development and optimization of acoustic bubble structures at high frequencies, Ultrason. Sonochem. 18 (1) (Jan. 2011) 92–98, https://doi.org/10.1016/j.ultsonch.2010.03.004.
[57] A.A. Gubaidullin, O.Y. Kuchugurina, D.M.J. Smeulders, C.J. Wisse, Frequency-dependent acoustic properties of a fluid/porous solid interface, J. Acoust. Soc. Am. 116 (3) (2004) 1474–1480, https://doi.org/10.1121/1.1777856.
[58] Ensminger, Dale, and Leonard J. Bond. Ultrasonics : Fundamentals, Technologies and Applications, Third Edition, CRC Press LLC, 2011. ProQuest Ebook Central, https://ebookcentral-proquest-com.ezproxy1.lib.asu.edu/lib/asulib-ebooks/detail.action?docID=767859.
[59] J.A. Gallego-Juarez, K.F. Graff, Power Ultrasonics: Applications of High-Intensity Ultrasound, Elsevier Science & Technology, Kent, United Kingdom, 2014.
[60] H. Kiani, D.-W. Sun, Z. Zhang, The effect of ultrasound irradiation on the convective heat transfer rate during immersion cooling of a stationary sphere, Ultrason. Sonochem. 19 (6) (2012) 1238–1245, https://doi.org/10.1016/j.ultsonch.2012.04.009.
[61] C. Bartoli, F. Baffigi, Effects of ultrasonic waves on the heat transfer enhancement in subcooled boiling, Exp. Therm Fluid Sci. 35 (3) (2011) 423–432, https://doi.org/10.1016/j.expthermflusci.2010.11.002.
[62] O. Bulliard-Sauret, et al., Heat transfer intensification by low or high frequency ultrasound: thermal and hydrodynamic phenomenological analysis, Exp. Therm Fluid Sci. 104 (2019) 258–271, https://doi.org/10.1016/j.expthermflusci.2019.03.003.
[63] G.L. Lee, M.C. Law, V.C.-C. Lee, Modelling of liquid heating subject to simultaneous microwave and ultrasound irradiation, Appl. Therm. Eng. 150 (2019) 1126–1140, https://doi.org/10.1016/j.applthermaleng.2019.01.064.
[64] K. Urano, Y. Koichi, Y. Nakazawa, Equilibria for adsorption of organic compounds on activated carbons in aqueous solutions I. Modified Freundlich isotherm equation and adsorption potentials of organic compounds, J. Colloid Interface Sci. 81 (2) (1981) 477–485, https://doi.org/10.1016/0021-9797(81)90429-X.
[65] M.H. Entezari, P. Kruus, Effect of frequency on sonochemical reactions II. Temperature and intensity effects, Ultrason. Sonochem. 3 (1) (1996) 19–24, https://doi.org/10.1016/1350-4177(95)00037-2.
[66] G. Cum, G. Galli, R. Gallo, A. Spadaro, Role of frequency in the ultrasonic activation of chemical reactions, Ultrasonics 30 (4) (1992) 267–270, https://doi.org/10.1016/0041-624X(92)90086-2.
[67] G.O.H. Whillock, B.F. Harvey, Ultrasonically enhanced corrosion of 304L stainless steel II: The effect of frequency, acoustic power and horn to specimen distance, Ultrason. Sonochem. 4 (1) (1997) 33–38, https://doi.org/10.1016/S1350-4177(96)00015-6.
[68] A. Weissler, Sonochemistry: the production of chemical changes with sound waves, J. Acoust. Soc. Am. 25 (4) (1953) 651–657, https://doi.org/10.1121/1.1907158.
[69] Z. Li, X. Li, H. Xi, B. Hua, Effects of ultrasound on adsorption equilibrium of phenol on polymeric adsorption resin, Chem. Eng. J. 86 (3) (2002) 375–379, https://doi.org/10.1016/S1385-8947(01)00301-1.